

# Template-Directed Architectural Isomerism of Open Molecular Frameworks: Engineering of Crystalline Clathrates

Jennifer A. Swift, Adam M. Pivovar, Anne M. Reynolds, and Michael D. Ward\*

Contribution from the Department of Chemical Engineering and Materials Science, University of Minnesota, Amundson Hall, 421 Washington Ave. S.E., Minneapolis, Minnesota 55455-0132

Received March 9, 1998

**Abstract:** Crystalline clathrates formed from two-dimensional guanidinium sulfonate hydrogen-bonded networks connected by 4,4'-biphenyldisulfonate "pillars" in the third dimension exhibit a "brick-like" molecular framework that is a predictable architectural isomer of a previously observed bilayer architecture based on the same pillars. The amount of void space in the brick framework is nominally twice that of the bilayer form, with the framework occupying only 30% of the total volume. The formation of the brick architecture can be attributed to steric templating by the included molecular guests and host-guest interactions that favor assembly of this framework over its bilayer counterpart. The brick framework conforms to the different steric demands and occupancies of various aromatic guests (1,4-dibromobenzene, 1-nitronaphthalene, nitrobenzene, and 1,4-divinylbenzene) by puckering of the flexible, yet resilient, hydrogen-bonded network and by rotation of the pillars about their long axes, the latter also governing the width of the pores in the framework. These observations demonstrate that crystal engineering, and the ability to direct architectural isomerism in porous molecular lattices by the appropriate choice of molecular guest, is simplified by the use of robust 2-D networks.

## Introduction

The de novo design of solid state structure and properties in molecular crystals, the principal goal of crystal engineering, commonly is frustrated by an inability to predict and control molecular organization in the crystalline state.<sup>1–3</sup> This is especially true for porous molecular lattices and related crystalline clathrates,<sup>4</sup> which are susceptible to polymorphism and the formation of alternative close-packed structures. Nevertheless, the promise of these materials in chemical separations, catalysis, optoelectronics, and magnetism has stimulated efforts to develop crystal engineering strategies for the synthesis of open host frameworks. These strategies typically rely on "programmed" assembly of host frameworks through carefully designed non-covalent interactions between topologically and chemically complementary functional groups of the host constituents. Clathrates based on metal coordination,<sup>5–8</sup> and hydrogen bonding,<sup>9–14</sup> networks exhibit open frameworks with topologies that reflect their metal-ligand coordination environments and

arrangement of hydrogen-bonding groups, respectively. However, reliable predictions of host network topologies can be elusive as these architectures generally are sensitive to minor changes in the molecular constituents<sup>15,16</sup> and polymorphism in clathrates can be unpredictable.<sup>17</sup>

The design and synthesis of open host frameworks can be further influenced by molecular guests. Although in many cases this involves subtle changes in the structure and dimensions of a host framework with retention of the general lattice architecture,<sup>18–20</sup> some host architectures are affected more significantly by guest structure. Tri-*o*-thymotide clathrates exhibit cage-like cavities for small guests but channel-type pores with long chain molecules.<sup>21,22</sup> Metal coordination networks can form different structures as a result of ligand conformational isomerism induced by inclusion of different solvent molecules.<sup>23</sup> Host lattices based on 1-D hydrogen-bonded chains of an-

(1) Desiraju, G. R. *Crystal Engineering: The Design of Organic Solids*; Elsevier: New York, 1989.

(2) Kitaigorodskii, A. I. *Molecular Crystals and Molecules*; Academic Press: New York, 1973.

(3) Gavezzotti, A. *Acc. Chem. Res.* **1994**, *27*, 309–314.

(4) Bishop, R. *Chem. Soc. Rev.* **1996**, 311–319.

(5) Venkataraman, D.; Lee, S.; Zhang, J.; Moore, J. S. *Nature* **1995**, *371*, 591–593.

(6) Melendez, R. E.; Sharma, C. V. K.; Zaworotko, M. J.; Bauer, C.; Rogers, R. D. *Angew. Chem., Int. Ed. Engl.* **1996**, *35*, 2213–2215.

(7) Aakeröy, C. B.; Nieuwenhuyzen, M. J. *Mol. Struct.* **1996**, *374*, 223–239.

(8) Yaghi, O. M.; Davis, C. E.; Li, G.; Li, H. J. *Am. Chem. Soc.* **1997**, *119*, 2861–2868.

(9) Ermer, O.; Lindenberg, L. *Helv. Chim. Acta* **1991**, *74*, 825–877.

(10) Brunet, P.; Simard, M.; Wuest, J. D. *J. Am. Chem. Soc.* **1997**, *119*, 2737–2738.

(11) Kolotuchin, S. V.; Fenton, E. E.; Wilson, S. R.; Loweth, C. J.; Zimmerman, S. C. *Angew. Chem., Int. Ed. Engl.* **1995**, *34*, 2654–

(12) Aoyama, Y.; Endo, K.; Anzai, T.; Yamaguchi, Y.; Tomoya, S.; Kobayashi, K.; Kanehisa, N.; Hashimoto, H.; Kai, Y.; Masuda, H. *J. Am. Chem. Soc.* **1996**, *118*, 5562–5571.

(13) Hollingsworth, M. E.; Brown, M. E.; Hillier, A. C.; Santasiero, B. D.; Chaney, J. D. *Science* **1996**, *273*, 1355–1359.

(14) Ramamurthy, V.; Eaton, D. *Chem. Mater.* **1994**, *6*, 1128–1136.

(15) Fujita, M.; Kwon, Y. J.; Sasaki, O.; Yamaguchi, K.; Ogura, K. *J. Am. Chem. Soc.* **1995**, *117*, 7287–7288.

(16) Sada, K.; Kondo, T.; Yasuda, Y.; Miyata, M.; Miki, K. *Chem. Lett.* **1994**, 727–730.

(17) Ung, A. T.; Bishop, R.; Craig, D. C.; Dance, I. G.; Scudder, M. L. *Tetrahedron Lett.* **1993**, *49*, 639–648.

(18) Hollingsworth, M. D.; Santasiero, B. D.; Harris, K. D. M. *Angew. Chem., Int. Ed. Engl.* **1994**, *33*, 649–652.

(19) Mak, T. C. W.; Wong, H. N. C. *Top. Curr. Chem.* **1987**, *140*, 141–164.

(20) Gdaniec, M.; Ibragimov, B. T.; Talipov, S. A. *J. Incl. Phenom. Mol. Recogn. Chem.* **1990**, *9*, 231–242.

(21) Gerdil, R. *Top. Curr. Chem.* **1987**, *140*, 72–105.

(22) Hulliger, J.; König, O.; Hoss, R. *Adv. Mater.* **1995**, *7*, 719–721.

(23) Hennigar, T. L.; MacQuarrie, D. C.; Losier, P.; Rogers, R. D.; Zarowotko, M. J. *Angew. Chem., Int. Ed. Engl.* **1997**, *36*, 972–973.

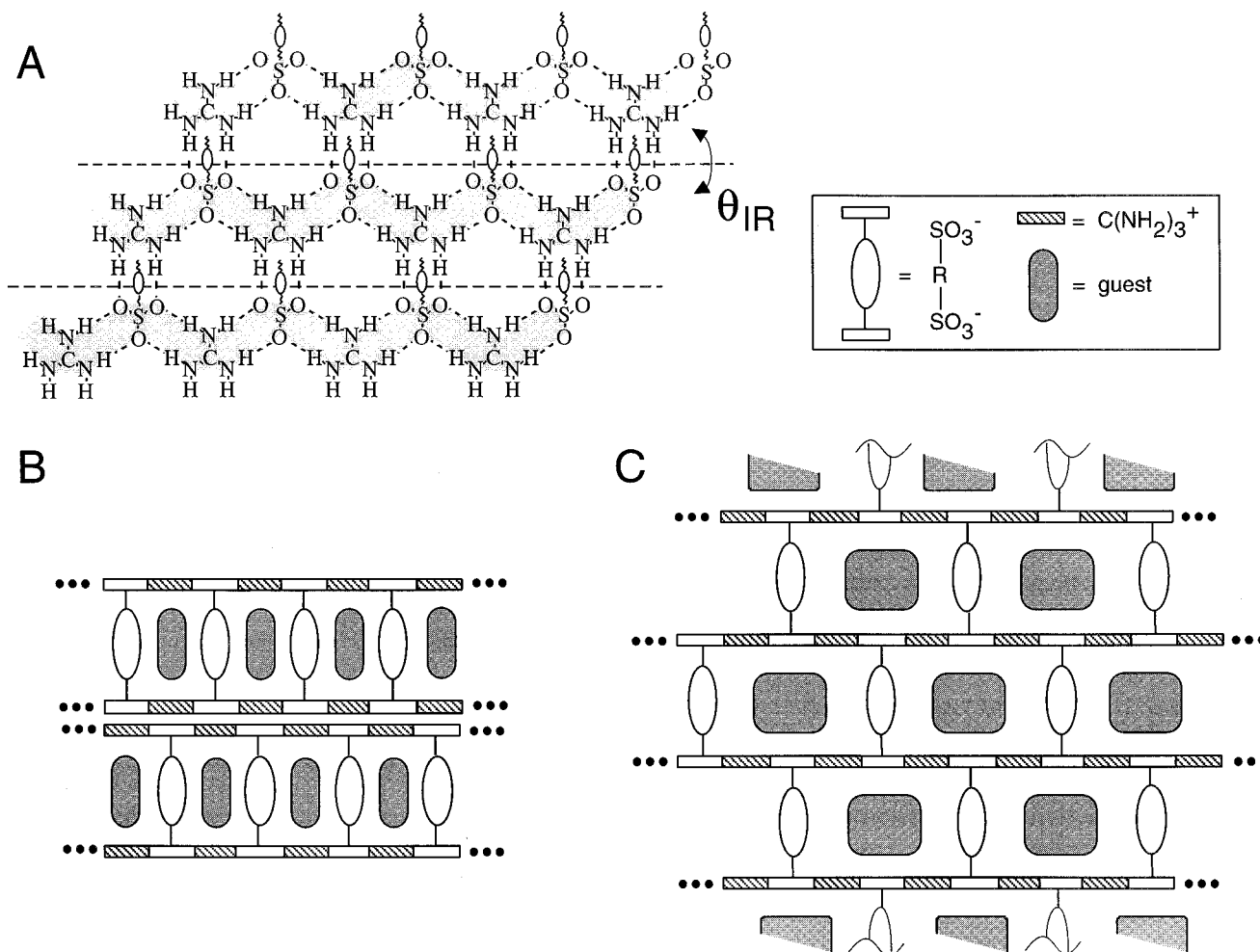


**Figure 1.** (A) Schematic representation of the quasi-hexagonal **GS** sheet. The one-dimensional **GS** ribbons are shaded gray and the horizontal dashed lines represent the axis about which the **GS** sheet puckers. The interribbon dihedral angle  $\theta_{IR}$  indicates the degree of puckering;  $\theta_{IR} = 180^\circ$  for a planar sheet. The disulfonate pillars in the bilayer motif are all oriented to the same side of the **GS** sheet, whereas their orientation in the brick motif alternates between adjacent ribbons. (B) Schematic representation of the pillared bilayer motif, illustrating the 1-D pores occupied by guest molecules. (C) Schematic representation of the pillared brick motif, illustrating the larger 1-D pores occupied by guest molecules. This architectural isomer can be conceptually generated by vertically shifting every other row of pillars in the bilayer motif so that the layers are continuously connected.

thracene–resorcinol derivatives form two types of inclusion architectures, with the selectivity for these structures dependent upon the nature of the guests.<sup>24</sup> This response of cavity size and host architecture to guest molecules is reminiscent of the templating role ascribed to small molecules and surfactant microstructures that influence the architecture of porous zeolites.<sup>25,26</sup>

Despite these advances, prediction of architectural isomers of open molecular frameworks and their structures remains difficult and typically is achieved only in hindsight. We previously demonstrated that numerous crystalline layered phases based on a 2-D hydrogen-bonded network of complementary guanidinium (**G**) and organosulfonate (**S**) ions, in which organic residues attached to the sulfonate moiety project from the surface of **GS** sheets, exhibit predictable structures (Figure 1).<sup>27–30</sup> The pervasiveness of the **GS** network was attributed

to its ability to adjust to the different steric requirements of various organic residues by puckering of the sheets and, for large organic residues, by alternating the projection of the sulfonate organic groups to opposite sides of the **GS** sheet. These observations demonstrated the benefits of crystal engineering approaches based on *flexible* 2-D networks that can tolerate differently sized ancillary groups.

Recently, we extended these concepts to crystalline host–guest clathrates based on **G** ions and organodisulfonates, the latter serving as molecular pillars that connect opposing **GS** sheets to generate bilayered open frameworks (Figure 1).<sup>31,32</sup> These frameworks were supported by pillars (e.g., 1,2-ethyl-, 1,4-butyl-, 2,6-naphthyl-, and 4,4'-biphenyldisulfonate) that flanked one-dimensional pores<sup>33</sup> occupied by a diverse variety of molecular guests. Notably, the dense 2-D **GS** network

(24) Endo, K.; Ezuhara, T.; Koyanagi, M.; Masuda, H.; Aoyama, Y. *J. Am. Chem. Soc.* **1997**, *119*, 499–505.

(25) Davis, M. E.; Katz, A.; Ahmad, W. R. *Chem. Mater.* **1996**, *8*, 1820–1839.

(26) Huo, Q.; Margolese, D. I.; Stucky, G. D. *Chem. Mater.* **1996**, *8*, 1147–

(27) Russell, V. A.; Etter, M. C.; Ward, M. D. *J. Am. Chem. Soc.* **1994**, *116*, 1941–1952.

(28) Russell, V. A.; Etter, M. C.; Ward, M. D. *Chem. Mater.* **1994**, *6*, 1206–1217.

(29) Russell, V. A.; Ward, M. D. *Acta Crystallogr.* **1996**, *B52*, 209–214.

(30) Russell, V. A.; Ward, M. D. *J. Mater. Chem.* **1997**, *7*, 1123–1133.

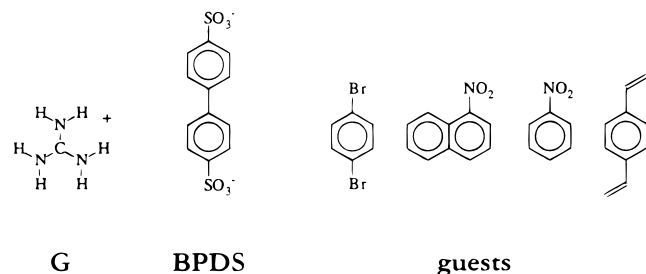
(31) Russell, V. A.; Evans, C. C.; Li, W.; Ward, M. D. *Science* **1997**, *276*, 575–579.

(32) Swift, J. A.; Russell, V. A.; Ward, M. D. *Adv. Mater.* **1997**, *9*, 1183–1186.

prohibited multifold interpenetration and the associated loss of framework porosity, a problem commonly encountered in crystalline clathrates and porous molecular frameworks.<sup>34–38</sup>

The resilience and fixed dimensionality of the **GS** networks prompted us to search for an isomer of these bilayer phases possessing a “brick” architecture. This isomer can be conceptually generated from the bilayer form by shifting every other row of the disulfonate pillars in a direction normal to the **GS** sheets so that all the sheets are continuously connected. We surmised that a brick isomer, which would have nominally twice the porosity of the bilayer for a given pillar, could be templated by guest molecules incapable of being included in the bilayer pores. The feasibility of the brick architecture for these various pillars is supported by clathrates prepared with 1,5-naphthalenedisulfonate pillars, which exhibit a highly puckered brick framework with linear molecules included in narrow one-dimensional pores. However, architectural isomerism has not been observed for the 1,5-naphthalenedisulfonate clathrates, apparently due to denser packing achieved in the brick form relative to its bilayered counterpart.<sup>39</sup>

We describe herein the synthesis and structure of brick frameworks constructed from guanidinium ions, the 4,4'-biphenyldisulfonate (**BPDS**) pillar and suitable guests (1,4-dibromobenzene, 1-nitronaphthalene, nitrobenzene, and 1,4-divinylbenzene) that demonstrate architectural isomerism for a compositionally identical host framework. The ability to access this architecture extends the inclusion behavior of the **GS** clathrates, which is crucial to the development and future utility of these materials.



## Experimental Section

**General Methods.** Single crystals of all guanidinium biphenyldisulfonate clathrates,  $(\text{G})_2(\text{BPDS}) \cdot n(\text{guest})$ , were grown at room temperature by slow evaporation of saturated methanol solutions containing 2:1 mixtures of guanidine hydrochloride (Aldrich, 99%) and 4,4'-biphenyldisulfonic acid (TCI), in the presence of the appropriate aromatic guest. The concentration of the solid guests 1,4-dibromobenzene (Aldrich, 98%) and 1-nitronaphthalene (Aldrich, 99%) was equivalent to that of **BPDS**, whereas an excess of the liquid guests nitrobenzene (Aldrich, 99%) and divinylbenzene (Aldrich, 80%) was used (~1 mL). All compounds were used as received without further purification. Gas chromatographic analysis indicated that the divinyl-

benzene reagent, as purchased, contained 26% 1,4-divinylbenzene, 55% 1,3-divinylbenzene, 10% 1,3-ethylvinylbenzene, and 9% 1,4-ethylvinylbenzene. Crystallization solutions typically contained a combined 200 mg of guanidine hydrochloride and 4,4'-biphenyldisulfonic acid in 5–10 mL of solvent. Single crystals grew as flat plates or thick needles with dimensions of all the faces typically exceeding 1 mm<sup>2</sup>.

**Physical Data. <sup>1</sup>H NMR Spectroscopy.** The composition of the clathrates was determined by <sup>1</sup>H NMR of d<sub>6</sub>-dmsO solutions prepared from isolated single crystals. <sup>1</sup>H NMR spectra were recorded either on a Varian INOVA 500 MHz or a Unity 300 MHz spectrometer. The host lattice constituents were identified by the resonances for the guanidinium ion ( $\delta = 6.93$ , 12 H, s) and the 4,4'-biphenyldisulfonate ion ( $\delta = 7.62$ –7.70, 8H, m). The guest identity and stoichiometry for each compound were confirmed by their chemical shifts and integrated peak areas:  $(\text{G})_2(\text{BPDS}) \cdot (1,4\text{-dibromobenzene})$  (**I**),  $\delta = 7.54$ , 4H, s;  $(\text{G})_2(\text{BPDS}) \cdot (1\text{-nitronaphthalene})$  (**II**),  $\delta = 8.00$ –8.42, 7H, m;  $(\text{G})_2(\text{BPDS}) \cdot 2(\text{nitrobenzene})$  (**III**),  $\delta = 8.23$ –8.26, 4H, d;  $\delta = 7.84$ , 2H, m;  $\delta = 7.64$ –7.72, 4H, mixed with **BPDS** resonances;  $(\text{G})_2(\text{BPDS}) \cdot 1.5\text{-}(1,4\text{-divinylbenzene})$  (**IV**),  $\delta = 5.26$ –5.37, m; 5.78–5.86, m; 6.71–6.81, m; 7.36–7.47. The <sup>1</sup>H NMR of dissolved **IV** was complex and indicated that each crystal contained a mixture of 1,4-divinylbenzene (75%), 1,3-divinylbenzene (17%), and 1,4-ethylvinylbenzene (8%) with a variance of  $\pm 2\%$ , confirmed by gas chromatographic analysis.

**X-ray Crystallography.** Experimental details of the X-ray analysis are provided in Table 1. All single-crystal X-ray data were collected (hemisphere technique) on a Siemens SMART Platform CCD diffractometer with graphite monochromated Mo K $\alpha$  radiation ( $\lambda = 0.71073$ ) at 173(2) K. The structures were solved by direct methods (SHELXTL-V5.0, Siemens Industrial Automation, Inc., Madison, WI) and refined using full-matrix least-squares/difference Fourier techniques. All non-hydrogen atoms were refined with anisotropic displacement parameters and all hydrogen atoms were placed in idealized positions and refined as riding atoms with the relative isotropic displacement parameters. Absorption corrections were applied with the Siemens Area Detector ABSorption program (SADABS).<sup>40</sup>

## Results and Discussion

**General Features of the  $(\text{G})_2(\text{BPDS})$  Bilayer and Brick Architectures.** Our previous studies of bilayer guanidinium organodisulfonate clathrates demonstrated that the pore size and selectivity toward guest inclusion depended upon the length and molecular volume of the chosen pillar. The length of the **BPDS** pillars in  $(\text{G})_2(\text{BPDS})$  bilayer host frameworks has enabled inclusion of over 25 different aromatic guests.<sup>31,41</sup> This versatility is largely due to an inherent flexibility of the framework that enables it to adjust to differently sized guests. This flexibility stems from several sources. The  $(\text{G})\text{N}-\text{H} \cdots \text{O}(\text{S})$  hydrogen bonds can rotate out of the **GS** plane with concomitant tilting of the **BPDS** pillars to allow the bilayer thickness to shrink to the dimensions of the guest molecule. Conformational twisting of the **BPDS** pillars about the central C–C and rotation about the carbon–sulfur bonds provide an additional mechanism for accommodating the steric demands of the guests.

The structure of  $(\text{G})_2(\text{BPDS}) \cdot (\text{naphthalene})$  is illustrative of the bilayer architecture (Figure 2).<sup>42</sup> The **GS** sheets in this compound actually adopt the “shifted ribbon motif”, which is closely related to the quasihexagonal motif depicted in Figure 1.<sup>43</sup> The naphthalene guests occupy pores oriented along the *a* axis that are flanked by planar **BPDS** pillars. The pores are

(40) Blessing, R. *Acta Crystallogr.* **1995**, *A51*, 33–38.

(41) Swift, J. A.; Ward, M. D.; Reynolds, A. M. Manuscript in preparation.

(42)  $(\text{G})_2(\text{BPDS}) \cdot \text{naphthalene}$  crystallizes in the  $P\bar{1}$  space group, with  $a = 6.1533$ ,  $b = 7.1738$ ,  $c = 14.584$ ,  $\alpha = 98.313^\circ$ ,  $\beta = 90.198^\circ$ ,  $\gamma = 93.657^\circ$ . The guest-free packing fraction of  $(\text{G})_2(\text{BPDS}) \cdot \text{naphthalene}$  is 0.52, and 0.71 with guest.

(33) The term “pore” is used here to describe the void space in the host framework that would exist if the guest were absent.

(34) Ermer, O. *J. Am. Chem. Soc.* **1988**, *110*, 3747–3754.

(35) Simard, M.; Su, D.; Wuest, J. D. *J. Am. Chem. Soc.* **1991**, *113*, 4696–4698.

(36) Copp, S. B.; Subramanian, S.; Zaworotko, M. J. *J. Am. Chem. Soc.* **1992**, *114*, 8719–8720.

(37) Reddy, D. S.; Craig, D. C.; Rae, A. D.; Desiraju, G. R. *J. Chem. Soc., Chem. Commun.* **1993**, 1737–1739.

(38) Batten, S. R.; Hoskins, B. F.; Robson, R. *J. Am. Chem. Soc.* **1995**, *117*, 5385–5386.

(39) Although molecular modeling suggested that a bilayer phase with the 1,5-naphthyldisulfonate pillars was feasible, the void spaces are not large enough to include guest molecules, even small ones such as methanol. This suggests that denser packing can be realized in the brick framework clathrates than in bilayers based on this pillar.

**Table 1.** Crystallographic Data for I–IV

	I	II	III	IV
formula	C <sub>20</sub> H <sub>24</sub> Br <sub>2</sub> N <sub>6</sub> O <sub>6</sub> S <sub>2</sub>	C <sub>24</sub> H <sub>27</sub> N <sub>7</sub> O <sub>8</sub> S <sub>2</sub>	C <sub>19</sub> H <sub>20</sub> N <sub>5</sub> O <sub>7</sub> S	C <sub>22</sub> H <sub>25</sub> N <sub>3</sub> O <sub>3</sub> S
FW	668.39	605.65	462.46	411.51
dimensions (mm <sup>3</sup> )	0.24 × 0.11 × 0.08	0.04 × 0.35 × 0.21	0.26 × 0.24 × 0.05	0.30 × 0.18 × 0.16
color, shape	colorless, plate	light yellow, plate	colorless, plate	colorless, plate
crystal system	monoclinic	orthorhombic	monoclinic	monoclinic
space group	<i>P</i> 2 <sub>1</sub> / <i>c</i>	<i>Pna</i> 2 <sub>1</sub>	<i>P</i> 2 <sub>1</sub> / <i>n</i>	<i>P</i> 2 <sub>1</sub> / <i>n</i>
<i>a</i> (Å)	15.3145(10)	15.7309(8)	7.6881(7)	7.6132(2)
<i>b</i> (Å)	7.5637(5)	7.3988(4)	9.9552(9)	11.4829(3)
<i>c</i> (Å)	23.903(2)	23.233(1)	29.215(3)	25.8044(7)
β (deg)	105.321(1)	—	94.127(2)	91.410(1)
volume (Å <sup>3</sup> )	2670.4(3)	2704.1(2)	2230.2(4)	2255.18(10)
<i>Z</i>	4	4	4	4
<i>D</i> <sub>calc</sub> (mg/m <sup>3</sup> )	1.663	1.488	1.377	1.212
<i>F</i> (000)	1344	1264	964	872
absorption coefficient (mm <sup>-1</sup> )	3.239	0.259	0.195	0.170
θ range for data (deg) collection	1.38–25.06	1.75–25.06	1.40–25.14	1.58–25.06
unique reflections	4660	3979	3911	3802
no. obs ( <i>I</i> > 2σ)	3225	3011	1980	2597
<i>R</i> , <sup>a</sup> <i>R</i> <sub>w</sub> <sup>b</sup>	0.0613, 0.1499	0.0524, 0.1022	0.0793, 0.1506	0.0843, 0.1786
GOF	1.020	1.033	1.009	1.035

<sup>a</sup>  $R = \sum ||F_o| - |F_c|| / \sum |F_o|$ . <sup>b</sup>  $R_w = [\sigma^2(F_o^2) + (AP)^2 + (BP)^2]^{-1/2}$ , where  $P = (F_o^2 + 2F_c^2)/3$ .

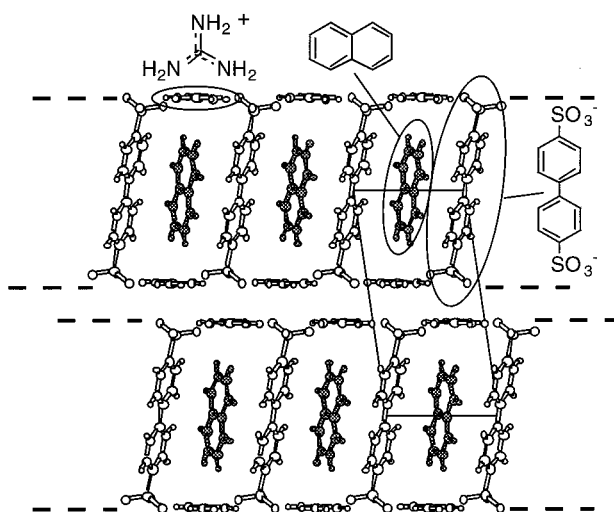


**Figure 2.** Molecular packing of (G)<sub>2</sub>(BPDS)·(naphthalene) as viewed along the *a* axis oriented 1-D pores. The pores are perpendicular to the GS ribbon direction, which are oriented horizontal in the plane of the page (indicated by the dotted lines).

nominally perpendicular to the GS ribbons in the 2-D network. The GS sheets are planar overall, but the sulfonate groups rotate slightly out of the mean GS plane so that the long axes of the BPDS pillars are tilted slightly.<sup>44</sup> The BPDS pillars are slightly rotated so that their molecular planes are not quite parallel to the pore direction.

We reported earlier that these characteristics—the shifted ribbon motif, pillar tilting, and pillar rotation—were common for the bilayer phases and reflected a structural flexibility that enables the host framework to conform to the guests and optimize host–guest interactions. Indeed, hydrogen atoms of the naphthalene guest molecules in (G)<sub>2</sub>(BPDS)·(naphthalene) project toward the center of the BPDS aromatic rings, suggesting (arene)C–H···π interactions that are common in solid-state structures of aromatic molecules, including naphthalene.<sup>45</sup>

(43) The shifted ribbon motif can be generated from the quasihexagonal form by a slight translational shift of the GS ribbons along the ribbon axis. This motif is characteristic of the bilayer phases prepared with BPDS pillars.

(44) The long axis of the BPDS pillar is tilted 10° and 12° with respect to an axis normal to the GS plane when viewed along the *a* and *b* axes, respectively. The BPDS pillars rotate about the C–S bonds to subtend an angle of 21.5° with the pore direction.

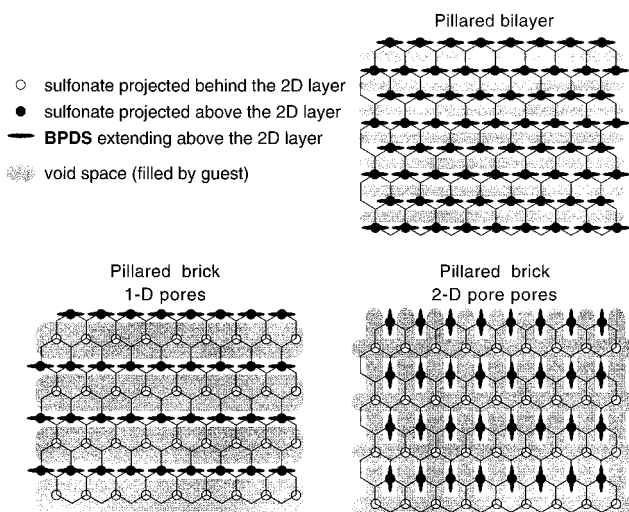


**Figure 3.** Schematic representations of the pores created in the pillared (G)<sub>2</sub>(BPDS) bilayer and brick phases as viewed normal to the GS network (the G ions of the upper layer are omitted). If the aromatic planes of the BPDS pillars in the bilayer motif are either perpendicular (not shown) or parallel to the ribbon direction, 1-D pores are formed. If the aromatic planes of the BPDS pillars are parallel to the ribbon direction in the brick motif, the width of the pores is nominally twice that of the bilayer because the pillars of adjacent GS ribbons alternate orientation about the GS sheet. In contrast, if the planes of the BPDS pillars are orthogonal to the ribbon direction a 2-D pore network is created.

Simple models of the gallery regions between the 2-D GS sheets illustrate the differences between the bilayer and brick architectures (Figure 3). The bilayer architecture can have 1-D pores, flanked by the aromatic planes of the BPDS pillars, parallel or perpendicular to the GS ribbons. The width of the pores is governed by the distance between adjacent rows of organodisulfonate pillars.

In the brick architecture, pillars on adjacent GS ribbons project to opposite sides of the GS sheet, nominally doubling the void space in the pores. The actual structure and dimensions

(45) (a) Hunter, C. A.; Sanders, J. K. M. *J. Am. Chem. Soc.* **1990**, *112*, 5525–5534. (b) Desiraju, G. R.; Gavezzotti, A. *J. Chem. Soc., Chem. Commun.* **1989**, 621–623. (c) Gavezzotti, A. *Chem. Phys. Lett.* **1989**, *161*, 67–72.

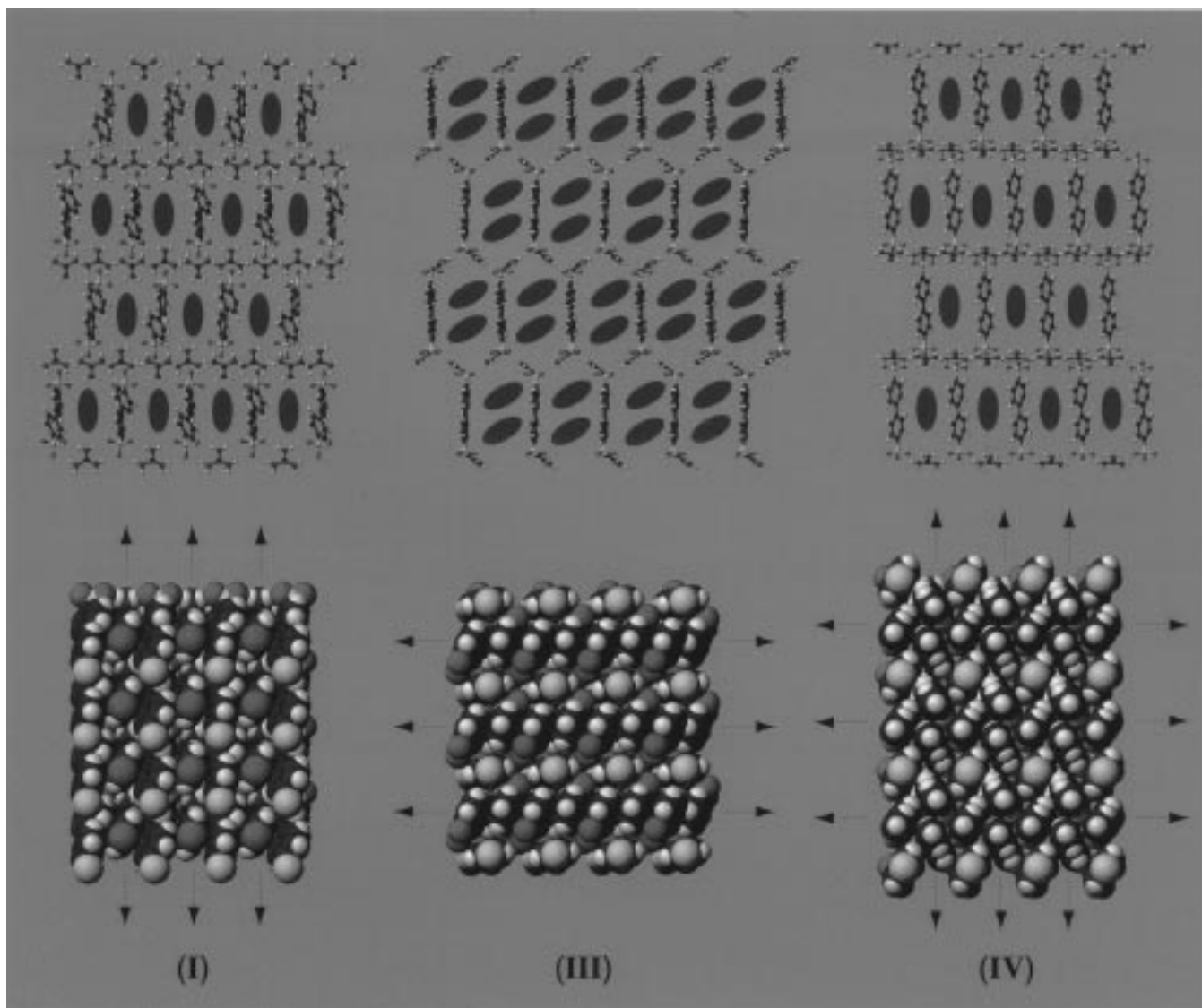


**Figure 4.** Molecular packing diagrams illustrating the brick host frameworks and guest occupancy of **I**, **III**, and **IV**. (top) Views along 1-D pores in each structure (the second pore in **IV** is not shown). The **GS** ribbons run left-to-right in **I** and **IV**, but are perpendicular to the plane of the paper in **III**. The purple ovals represent the guest molecules. One-half of the 1,4-divinylbenzene guests in **IV** reside on positions eclipsed by the **BPDS** pillars, but these have been omitted for clarity. (bottom) The corresponding space-filling diagrams for **I**, **III**, and **IV** depicting the arrangement of guests in the pores as viewed normal to the 2-D **GS** sheets. The pore directions are denoted by arrows. The **GS** ribbons are oriented horizontally in each diagram. The **G** ions and sulfonate oxygens of the top layer have been omitted so that the guests can be viewed. Atom colors: carbon (gray), hydrogen (white), nitrogen (blue), oxygen (red), sulfur (yellow); bromine (red).

of the pores in the brick architecture will depend on the orientation of **BPDS** pillar with respect to the ribbon direction and the tilt of the pillars. If the **BPDS** planes are parallel to the **GS** ribbons the pore width is determined by the separation between organodisulfonate ions in every other ribbon. This distance is  $\sim 15$  Å (compared with 7.5 Å in the bilayer architecture), the actual pore width depending upon the van der Waals thickness of the pillars. In contrast, if the **BPDS** planes are perpendicular to the ribbon direction a 2-D pore network with nominal pore widths of approximately 7.5 Å is expected. Consequently, the brick framework has the ability to accommodate larger guests or a higher occupancy of guest molecules.

The **BPDS** pillars in the brick framework are free to rotate and twist (about the central **BPDS** C–C bond) in order to adjust to the steric requirements of guests. The framework also can adapt to different guest molecules and occupancies by puckering of the **GS** sheet, which allows tilting of the **BPDS** pillar so that the host can conform to the guest. Molecular models reveal that this mode of puckering, in which both **G** and **S** ions are

rotated out of the mean **GS** plane, is prevented in the bilayered  $(\text{G})_2(\text{BPDS})$  clathrates by steric interactions between adjacent pillars. The slight pillar tilt observed in the bilayer phases actually is achieved by a small rotation of the sulfonate group out of the mean **GS** plane rather than by puckering. The **BPDS** pillars in the bilayers form a nearly close-packed wall along the channels if oriented normal to the sheet and reach the repulsive limit at tilt angles of approximately  $10^\circ$ . In contrast, the larger separation between pillars in the brick architecture allows significant tilting through true puckering of the **GS** sheet.

**Synthesis of Brick Frameworks.** Slow evaporation of methanol solutions containing 2:1 mixtures of guanidinium chloride and 4,4-biphenyldisulfonic acid and either 1,4-dibromobenzene, 1-nitronaphthalene, nitrobenzene, or divinylbenzene afforded plate-shaped crystals with the compositions  $(\text{G})_2(\text{BPDS}) \cdot (1,4\text{-dibromobenzene})$  (**I**),  $(\text{G})_2(\text{BPDS}) \cdot (1\text{-nitronaphthalene})$  (**II**),  $(\text{G})_2(\text{BPDS}) \cdot 2(\text{nitrobenzene})$  (**III**), and  $(\text{G})_2(\text{BPDS}) \cdot 1.5(1,4\text{-divinylbenzene})$  (**IV**), respectively. Crystallization of these phases was favored over formation of the methanol

**Table 2.** Summary of Structural Features for **I–IV**

	<b>I</b>	<b>II</b>	<b>III</b>	<b>IV</b>
GUEST	1,4-dibromobenzene	1-nitronaphthalene	nitrobenzene	1,4-divinylbenzene
<i>n</i>	1	1	2	1.5
PF (without guest) <sup>a</sup>	0.50	0.49	0.29	0.29
PF (with guest) <sup>a</sup>	0.67	0.71	0.65	0.64
<b>BPDS</b> (deg)	24.6	33.9	0	0
conformational twist				
<b>BPDS</b> tilt angle <sup>b</sup> (deg)	48	47	0	15
$\theta_{\text{IR}}$ <sup>c</sup> (deg)	63	62	103	130
pore direction	<i>b</i>	<i>a</i>	<i>a</i>	<i>a,b</i>
estimated pore aperture dimensions <sup>d</sup> (height × width in Å)	7.1 × 7.7	7.1 × 7.4	10.7 × 10.0	10.2 × 11.5 10.2 × 7.6
estimated maximum pore dimensions <sup>e</sup> (height × width in Å)	11.5 × 7.7	11.6 × 7.4	14.6 × 10.0	12.9 × 11.5 12.9 × 7.6

<sup>a</sup> PF = packing fraction, calculated by Connolly surfaces using Cerius<sup>2</sup> molecular modeling software (version 1.6). A comparison of arbitrarily chosen examples from the Cambridge Structural Database revealed that the PF values calculated with Cerius<sup>2</sup> are systematically lower, by an average of 1.2%, than the  $C_k$  values reported by others (see A. I. Kitaigorodskii *Molecular Crystals and Molecules* Academic Press: New York, 1973 and A. Gavezzotti *Nouv. J. Chim.* **1982**, 6, 443). <sup>b</sup> **BPDS** tilt angle is the angle between the long axis of **BPDS** and the normal to the **GS** mean plane. <sup>c</sup>  $\theta_{\text{IR}}$  = interribbon puckering angle, defined by the mean planes of guanidinium ions in adjacent ribbons. <sup>d</sup> Pore aperture dimensions were estimated from the center-to-center distance between appropriate sulfonate sulfur atoms as viewed normal to the pore cross section. The actual values will be smaller if the van der Waals radii are used. <sup>e</sup> Maximum pore dimensions are equivalent to  $c/2$ , which represents the maximum height of pore.

solvate, which exhibits a bilayer architecture.<sup>31</sup> We have observed a similar preference for inclusion of aromatic guests by the bilayer phases.

Single-crystal X-ray diffraction revealed that compounds **I–IV** each crystallized in the brick architecture with the **GS** sheets adopting the quasihexagonal motif, in contrast to the shifted ribbon motif observed for their bilayer counterparts. Guest molecules are included in pores that exist between the **GS** sheets (Figure 4) and can be expelled from the host lattice (or polymerized in the case of 1,4-divinylbenzene) by heating to temperatures exceeding 150°. Differences in puckering angle between ribbons in the **GS** sheet ( $\theta_{\text{IR}}$ ), interlayer separations, pillar tilt, pillar conformation, and guest occupancy can be attributed to the different steric requirements of the guests and host–guest interactions (Table 2). Puckering of the **GS** sheets leads to pores that are “corrugated”, described by a set of minimum (i.e., the pore aperture) and maximum pore dimensions.

The host frameworks of **I** and **II** are surprisingly similar. One-dimensional pores that are orthogonal to the **GS** ribbons are flanked by the **BPDS** pillars and occupied by the 1,4-dibromobenzene and 1-nitronaphthalene guest molecules, respectively. The **GS** network is highly puckered in each compound and the **BPDS** pillars in **I** and **II** are tilted substantially, thereby blocking the pore direction along the **GS** ribbon axis that otherwise would be accessible to guests if the pillars were vertical. In each case the guest molecules are organized along the pores such that the **BPDS** pillars and guests are close-packed.

The puckering of the (G)<sub>2</sub>(BPDS) framework and the accompanying pillar tilting in **I** and **II** results in a smaller amount of void space (guest-free) than predicted for the model brick framework with vertical pillars. In contrast to bilayered (G)<sub>2</sub>(BPDS)·(naphthalene), the phenyl rings of the **BPDS** pillar are not coplanar. This may reflect the ability of the lattice to conform further to the guest shape, or may be due to void regions not filled by the guests that simply allow the **BPDS** rings to twist and reduce otherwise repulsive *ortho* hydrogen interactions.<sup>46</sup> The different values of conformational twist observed in **I** and **II** can be ascribed to the different molecular shapes of the 1,4-dibromobenzene and 1-nitronaphthalene guests.

(46) Brock, C. P.; Minton, R. P. *J. Am. Chem. Soc.* **1989**, 111, 4586–4593.

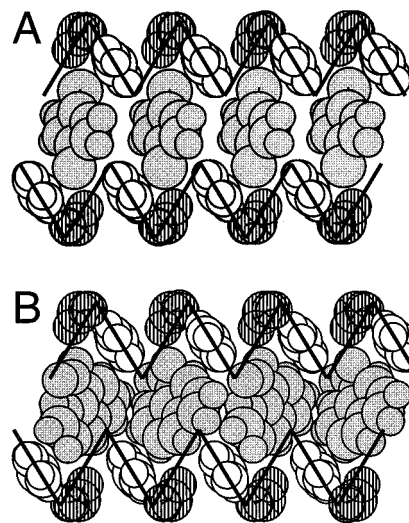


**Figure 5.** View normal to the 1-D pores in (a) **I** and (b) **II**, illustrating the puckering of the **GS** sheets and guest organization. The Br atoms of 1,4-dibromobenzene and nitro groups of 1-nitronaphthalene project into “pockets” created by the puckering, with identifiable close intermolecular contacts with the guanidinium cations. The puckering, depicted by the solid black lines, is defined by the mean planes of the guanidinium ions. Guest molecules (gray), guanidinium ions (white), SO<sub>3</sub> groups (shaded with the organic residue omitted for clarity).

Parallel studies in our laboratory have demonstrated that 1,4-dimethylbenzene and 1,4-bromotoluene guests promoted the formation of bilayer frameworks even though these guests have molecular volumes comparable to 1,4-dibromobenzene. Inspection of the structure of **I** reveals that the C–Br bonds of the 1,4-dibromobenzene guests in **I** are oriented vertically with the Br substituents directed away from the aromatic **BPDS** pillars.<sup>47</sup> The Br substituents are nestled in collapsed “pockets” of the corrugated pores that result from puckering the hexagonal **GS** sheets (Figure 5), with close packing between the aromatic planes of the guests and the **BPDS** pillars. Additionally, each Br substituent exhibits four different short contacts (<4 Å) to guanidinium nitrogen atoms in these pockets. Particularly short

(47) The asymmetric unit contains two **G**, one **BPDS**, and two halves of two independent guest molecules. The bromine atom on one of the guests is disordered about two sites, which have refined occupancies of 0.88 and 0.12. Text discussions pertain to the high occupancy Br position.

contacts for (G)N3···Br1 (3.48 Å) and (G)N5···Br2 (3.57 Å) are present, but the N—H···Br distances range from 3.24 to 3.31 Å with N—H···Br angles ranging from 96.2° to 102.7°, based on the calculated hydrogen positions for a planar guanidinium ion.

These structural features argue that N—H···Br hydrogen bonding does not drive formation of the brick architecture. Rather, this architecture may form as a consequence of an increased number of van der Waals contacts between the Br substituent and the host framework within the collapsed pockets, which cannot form in the bilayer. The presence of two Br substituents, which are more polarizable than the methyl groups of 1,4-dimethylbenzene and 1,4-bromotoluene, may be sufficient to drive the selectivity toward the brick framework.

The brick framework in **II** may be due to steric templating by the large 1-nitronaphthalene guests, as the structure of (G)<sub>2</sub>-(BPDS)·naphthalene suggests that the naphthalene guests are near the steric limit that can be accommodated by the bilayer phase. However, close host—guest (G)N—H···O(nitro) contacts (N4···O8 = 2.97 Å) are apparent in collapsed pockets of the GS sheets, which are structurally identical to the pockets observed in **I**. Hydrogen bonding interactions in **II** are suggested by N—H···O(nitro) bond distances of 2.72 Å, on the basis of the calculated H positions, but the N—H···O(nitro) H-bonding geometry is nonideal (N4—H4c···O8 = 97.2°). Nevertheless, N—H···O(nitro) hydrogen bonds can be relatively strong with calculated energies of ~15 kJ mol<sup>-1</sup>.<sup>48</sup> Rotation of the (G)C—NH<sub>2</sub> bond out of planarity (perhaps even dynamically) can afford a more linear H-bonding geometry, but deplanarizing the G ion is energetically costly. Interestingly, the nitro groups of the guest orient in the same direction throughout the crystal, resulting in a noncentrosymmetric space group and a net polar clathrate.

The aromatic planes of the guests are nominally parallel to the BPDS pillar planes in **I** and **II** and no C—H···π herringbone interactions are evident. In the case of **I** the aromatic rings of the 1,4-dibromobenzene guests are centered over the central C—C bonds of the BPDS pillar, whereas in **II** the nitrobenzene rings exhibit face-to-face π—π interactions with the pillars. We surmise that the electron withdrawing nature of the Br and nitro substituents reduces the repulsion between the aromatic π systems to make these packing motifs less unfavorable.

Clearly, the selectivity for these architectures reflects a delicate balance of energetic terms and is very sensitive to small steric differences or specific host—guest interactions. Interestingly, the guest-free packing fractions of **I** and **II** (that is, the amount of space occupied by the framework alone) is comparable to the values for the 1,4-dimethylbenzene, 1,4-bromotoluene, and naphthalene clathrates.<sup>40,49</sup> The ability of the brick framework to achieve low packing fractions stems from its inherent flexibility, which allows it to “shrink wrap” around the guests for optimized packing and make it an energetically accessible alternative to the bilayer phase. In the absence of this property (that is, if the network were rigid with the pillars fixed vertically) crystallization of the brick framework would be unfavorable, owing to the excessive void space that would be present.

In contrast to **I** and **II**, the BPDS pillars in **III** are rotated such that their planes are *parallel* to the GS ribbon direction. This affords large 1-D pores along the ribbon direction that are

occupied by “double-decker” π-stacks of nitrobenzene molecules in which the dipoles of neighboring nitrobenzene within a π-stack are antiparallel.<sup>50</sup> The GS sheet is puckered differently than in **I** and **II**; the pillars remain vertically oriented and only the G ions rotate out of the mean plane of the GS network. As a consequence of this puckering mode and the vertical pillar orientation, this host framework has a very low guest-free packing fraction of 0.29. The linear packing density of the nitrobenzene molecules along the π-stacks (2 molecules per 7.68 Å repeat) is similar to that observed in the low-temperature crystal structure of pure nitrobenzene (1 molecule per 3.86 Å repeat)<sup>51</sup> and other nitrobenzene derivatives.<sup>52</sup> Although nitrobenzene molecules would fit edgewise in the narrower pores of the (G)<sub>2</sub>(BPDS) bilayer architecture, the small width of the bilayer pores would prevent the formation of π-stacks in which the cross section of the molecule spans the pore width. This suggests that the formation of the brick architecture in **III** may be a consequence of templating by nitrobenzene π-stacked aggregates with the optimum antiparallel dipole—dipole arrangement. Close contacts between the nitrobenzene guests and the GS sheet (nitro-O···N(G), 3.08–3.34 Å) and (nitrobenzene)-C—H···π(BPDS) contacts also suggest favorable host—guest interactions that can stabilize the brick framework.

The clathrate **IV** was crystallized from solutions containing a mixture of divinylbenzene and ethylvinylbenzene isomers. However, each individual single crystal of **IV** contained a mixture of these structurally similar isomers, with 1,4-divinylbenzene predominating (75% vs 26% of the starting material, indicating an enrichment of this compound by clathration). The crystal structure of **IV** was solved with the major guest component, 1,4-divinylbenzene. The asymmetric unit refined as one 1,4-divinylbenzene molecule in a *cis* conformation and one-half of a 1,4-divinylbenzene molecule in the *trans* conformation sitting on an inversion center (work to obtain clathrates of the other compounds and isomers is in progress). Although the quality of the crystal structure of **IV** suffered from poor refinement of guest molecules, the structure of the host framework deduced from the X-ray data is reliable.

The host framework of **IV** can be considered as intermediate between those of **I/II** and **III**. Rather than orienting parallel or perpendicular to the 1-D pores, the planes of the BPDS pillars are rotated by 60° with respect to the GS ribbons. This affords two accessible orthogonal pores that are filled by a continuous 2-D array of divinylbenzene guest molecules, with a guest occupancy exceeding that of **I** and **II**. Each BPDS pillar is surrounded by six divinylbenzene guest molecules. Guest—guest, guest—pillar, and pillar—guest (arene)C—H···π interactions are readily apparent. The guest-free packing fraction of the framework is comparable to that of **III** as the pillars tilt only slightly. The absence of heteroatoms in 1,4-divinylbenzene argues that the formation of the brick architecture can be attributed to steric templating, as the smaller styrene molecule forms a bilayered clathrate. Interestingly, when crystals of **IV** are heated above 150° the guest is not expelled from the lattice. Rather, the divinylbenzene guests polymerize, presumably forming a highly cross-linked replica of the BPDS pillar network. Preliminary experiments indicate that the host can be removed by soaking single crystals in methanol to yield a polymeric material mimicking the original crystal morphology.<sup>53</sup>

(48) Allen, F. H.; Baalham, C. A.; Lommerse, J. P. M.; Raithby, P. R.; Sparr, E. *Acta Crystallogr.* **1997**, *B53*, 1017–1024.

(49) For example, the guest-free packing fractions of bilayer structures (G)<sub>2</sub>(BPDS)·1,4-bromotoluene and (G)<sub>2</sub>(BPDS)·1,4-dimethylbenzene are 0.52 and 0.53, respectively.

(50) Refinement of (III) was accomplished by fitting most of the 50 worst reflections to a minor twin component (~13% of the total crystal).

(51) Trotter, J. *Acta Crystallogr.* **1959**, *12*, 884–888.

(52) Andre, I.; Foces-Foces, C.; Cano, F. H.; Martinez-Ripoll, M. *Acta Crystallogr.* **1997**, *B53*, 984–995 and references therein.

(53) Pivovar, A. M.; Ward, M. D. Manuscript to be submitted.

## Conclusions

These observations clearly illustrate the influence of guest molecules on the architecture of open molecular frameworks. We have yet to observe both bilayer and brick architectures for the same guest molecule. This argues that the guest molecules serve as highly selective templates during the assembly of these host frameworks through steric effects and specific host–guest interactions. Although architectural isomerism in molecular networks has been demonstrated in a limited number of clathrate systems based on metal coordination, hydrogen bonding, and van der Waals networks, the guanidinium disulfonate system is unique in that the solid-state structure of the architectural isomers is highly predictable, largely because of the resilience of the 2-D **GS** network.

The pervasiveness of the **GS** architectures for a diverse variety of pillars and guests reflects their ability to conform to molecular guests and achieve dense packing. This adaptability and the

resilience of the 2-D **GS** network substantially simplifies crystal engineering and suggests significant opportunities for applications in which porous frameworks and clathrates have unique advantages in materials synthesis and processing.

**Acknowledgment.** The authors gratefully acknowledge the assistance of Victor G. Young, Jr. of the X-ray Crystallographic Laboratory at the University of Minnesota. A.M.R. acknowledges financial support from the National Science Foundation Research and Education Undergraduate Program.

**Supporting Information Available:** Tables of X-ray data collection/refinement parameters, atomic position parameters, anisotropic displacement parameters and thermal ellipsoid plots for **I–IV** and **(G)<sub>2</sub>(BPDS)·(naphthalene)** (25 pages, print/PDF). See any current masthead page for ordering information and Web access instructions.

JA980793D